NCTU-HEP-9902

Neutrino-photon scattering and its crossed processes in a background magnetic field

Tzuu-Kang Chyi[a], Chien-Wen Hwang[a], W. F. Kao[a], Guey-Lin Lin[a], Kin-Wang Ng[b], Jie-Jun Tseng[a]

[a]Institute of Physics, National Chiao-Tung University, Hsinchu, Taiwan

[b]Institute of Physics, Academia Sinica, Taipei, Taiwan

(February 1, 2008)

Abstract

We study the neutrino-photon processes such as $\gamma\gamma \to \nu\bar{\nu}$, $\nu\gamma \to \nu\gamma$, and $\nu\bar{\nu} \to \gamma\gamma$ in a background magnetic field smaller than the critical magnetic field $B_c \equiv m_e^2/e$. Using Schwinger's formalism, we extract leading magnetic-field contributions to the above processes. Our result is valid throughout the kinematic regime where both neutrino and photon energies are significantly smaller than m_W. We briefly discuss the astrophysical implications of our result.

PACS numbers: 13.25.Hw, 13.40.Hq

The relevance of neutrino-photon interactions in astrophysics and cosmology has been studied extensively [1]. For example, the plasmon decay $\gamma^* \to \nu\bar{\nu}$ in horizontal branch stars and red giants leads to a strong constraint on the neutrino magnetic-moment [2]. Similarly, the decay process $\nu' \to \nu\gamma$ was also calculated [3], and its partial width has been constrained by various astrophysical observations [1]. It is natural to ask whether the two-photon processes such as the scatterings $\gamma\gamma \to \nu\bar{\nu}$, $\nu\gamma \to \nu\gamma$ or the decay $\nu' \to \nu\gamma\gamma$ are also relevant in astrophysics and cosmology. It turns out that, due to the left-handedness of the weak interaction, the $O(G_F)$-contributions to the amplitudes of the above processes are proportional to the mass of the neutrino [4]. Hence the resulting cross sections or decay rates are very suppressed. On the other hand, similar processes involving three photons such as $\gamma\gamma \to \nu\bar{\nu}\gamma$ or $\nu\gamma \to \nu\gamma\gamma$ are not suppressed by the same mechanism [5]. Consequently, one expects that the cross sections for $\gamma\gamma \to \nu\bar{\nu}$ and its crossed processes should be enhanced under a strong background magnetic field. In fact, under a background magnetic field B, the cross section $\sigma(\gamma\gamma \to \nu\bar{\nu})$ with photon energy $E_\gamma \ll m_e$ is enhanced by a factor $(m_W/m_e)^4(B/B_c)^2$ [6] as compared to its counterpart in the vacuum, where m_W and m_e are the W boson and the electron masses respectively; $B_c \equiv m_e^2/e$ is the critical magnetic field.

The previous calculation on $\gamma\gamma \to \nu\bar{\nu}$ [6] applies an effective Lagrangian for $\gamma\gamma \to \nu\bar{\nu}\gamma$ [5] and replaces one of the external photon with the classical magnetic field. It is clear that such an approach is valid only in the limit that $E_\gamma,\ E_\nu \ll m_e$. In this work, we shall extend the previous analysis by studying the processes $\gamma\gamma \to \nu\bar{\nu}$, $\gamma\nu \to \gamma\nu$ and $\nu\bar{\nu} \to \gamma\gamma$ with E_γ and E_ν larger than m_e but still considerably smaller than m_W. This generalization is motivated by the fact that the above processes may take place in stars with temperatures higher than m_e. In this case, the effective-Lagrangian approach is no longer appropriate.

Let us begin with the process $\gamma\gamma \to \nu\bar{\nu}$ in a background magnetic field. For convenience, the cross section of this process is denoted as $\sigma_B(\gamma\gamma \to \nu\bar{\nu})$. The relevant Feynman diagram is depicted in Fig. 1. The effective four-fermion interactions between leptons and neutrinos can be written as

$$\mathcal{L} = -\frac{G_F}{\sqrt{2}} \left(\bar{\nu}_l \gamma_\alpha (1-\gamma_5)\nu_l\right) \left(\bar{e}\gamma^\alpha (g_V - g_A\gamma_5)e\right), \tag{1}$$

where $g_V = 1/2 + 2\sin^2\theta_w$ and $g_A = 1/2$ for $l = e$; $g_V = -1/2 + 2\sin^2\theta_w$ and $g_A = -1/2$ for $l = \mu, \tau$. We should remark that the contribution due to g_A is proportional to the neutrino mass in the limit of vanishing magnetic field. At $O(B)$ in the limit $B \ll B_c$, it gives no contribution to the amplitude by the charge conjugation invariance. Therefore we shall neglect the contribution by g_A. Likewise, we shall also neglect contributions by g_V for $l = \mu, \tau$, since $-1/2 + 2\sin^2\theta_w = 0.04 \ll 1$. The amplitude for $\gamma(k_1)\gamma(k_2) \to \bar{\nu}(p_1)\nu(p_2)$ in a background magnetic field reads:

$$\begin{aligned} M = & \frac{G_F g_V}{\sqrt{2}} 4\pi\alpha \bar{u}(p_2)\gamma^\rho(1-\gamma_5)v(p_1) \\ & \times \int d^4V d^4W tr\left[\gamma_\rho \mathcal{G}(W)\gamma_\nu \mathcal{G}(-V-W)\gamma_\mu \mathcal{G}(V)\right] \epsilon^\mu(k_1)\epsilon^\nu(k_2) \\ & \times \exp(\frac{-ie}{2} V^\lambda F_{\lambda\kappa} W^\kappa) \exp\left(i(k_1 V - k_2 W)\right) + (k_1, \mu \longleftrightarrow k_2, \nu), \end{aligned} \tag{2}$$

where $V = z - x$, and $W = x - y$; $\epsilon(k_1)$ and $\epsilon(k_2)$ are polarization vectors of the photons; $\mathcal{G}(W) \equiv \mathcal{G}(x-y)$ is a part of the full electron propagator $G(x,y)$ which has

the following form under a constant magnetic field [7] $G(x,y) = \Phi(x,y)\mathcal{G}(x-y)$, with $\Phi(x,y) = \exp\left\{ie\int_y^x d\xi^\mu \left[A_\mu + \frac{1}{2}F_{\mu\nu}(\xi-y)^\nu\right]\right\}$ and

$$\begin{aligned}\mathcal{G}(x-y) \equiv \mathcal{G}(W) = -i(4\pi)^{-2}\int_0^\infty \frac{ds}{s^2}\frac{eBs}{\sin(eBs)}\exp(-im_e^2 s + ieBs\sigma_3) \\ \times \exp\left[\frac{-i}{4s}(W_\parallel^2 + eBs\cot(eBs)W_\perp^2)\right] \\ \times \left[m_e + \frac{1}{2s}\left(\gamma\cdot W_\parallel + \frac{eBs}{\sin(eBs)}e^{-ieBs\sigma_3}\gamma\cdot W_\perp\right)\right],\end{aligned} \tag{3}$$

where $W^\mu = W_\parallel^\mu + W_\perp^\mu$ with $W_\perp^0 = 0$ and $\vec{W}_\perp\cdot\vec{B} = 0$, and $\sigma_3 = \begin{pmatrix}\boldsymbol{\sigma_3} & \mathbf{0}\\ \mathbf{0} & \boldsymbol{\sigma_3}\end{pmatrix}$ with $\boldsymbol{\sigma_3}$ the third Pauli matrix. We note that the overall phase $\Phi(x,y)$ breaks the translation invariance, which results from the existence of a constant magnetic field. The total phase of the three electron-propagators is summarized in the factor $\exp(-\frac{ie}{2}V^\lambda F_{\lambda\kappa}W^\kappa)$. This phase is easily obtained by realizing that the combination $d\xi^\mu(A_\mu + \frac{1}{2}F_{\mu\nu}\xi^\nu) \equiv \mathcal{A}$ in the expression for $\Phi(x,y)$ is an exact form which satisfies $\mathcal{A} = d\omega$. Therefore the integration of $\mathcal{A}$ around a closed loop vanishes. The total phase of the electron propagators is then given by

$$\Phi(x,y)\cdot\Phi(y,z)\cdot\Phi(z,x) = \exp(-\frac{ie}{2}V^\mu F_{\mu\nu}W^\nu). \tag{4}$$

For a constant magnetic field along $+z$ direction, we have $F_{12} = -F_{21} = B$ while other components of $F_{\mu\nu}$ vanish.

At this stage, the calculation of M remains nontrivial since the function $\mathcal{G}$ as given by Eq. (3) is complicated. To find a simplification for $\mathcal{G}$, we go to the momentum space, which amounts to writing $\mathcal{G}(x,y) = \int\frac{d^4p}{(2\pi)^4}e^{-ip(x-y)}\mathcal{G}(p)$, with

$$\begin{aligned}\mathcal{G}(p) = \int_0^\infty \frac{ds}{\cos(eBs)}\exp\left[-is\left(m_e^2 - p_\parallel^2 - \frac{\tan(eBs)}{eBs}p_\perp^2\right)\right] \\ \times\left[e^{ieBs\sigma_3}(m_e + \gamma\cdot p_\parallel) + \frac{\gamma\cdot p_\perp}{\cos(eBs)}\right].\end{aligned} \tag{5}$$

It is useful to write $\mathcal{G}$ in terms of Landau levels [8]

$$\mathcal{G}(p) = \sum_{n=0}^\infty \frac{-id_n(\alpha)(\gamma\cdot p_\parallel + m_e + \gamma\cdot p_\perp) + d_n'(\alpha)\gamma_1\gamma_2(m_e + \gamma\cdot p_\parallel)}{p_L^2 + 2neB} + i\frac{\gamma\cdot p_\perp}{p_\perp^2}, \tag{6}$$

where $p_L^2 = m_e^2 - p_\parallel^2$, $\alpha = -p_\perp^2/eB$, and $d_n(\alpha) = (-1)^n e^{-\alpha}(L_n(2\alpha) - L_{n-1}(2\alpha))$ with L_n the Laguerre polynomials. As indicated by Eq. (6), the B dependence of $\mathcal{G}(p)$ resides in $d_n(\alpha)$, $d_n'(\alpha)$, and the propagator $1/(p_L^2 + 2neB)$. For $B \ll B_c$, the propagator $\mathcal{G}$ and the phase factor $\exp(\frac{-ie}{2}V^\lambda F_{\lambda\kappa}W^\kappa)$ can be expanded in powers of eB. To the linear order in eB, we have [9]

$$\mathcal{G}(p) = i\frac{\gamma\cdot p + m_e}{p^2 - m_e^2 + i\epsilon} - \frac{\gamma^1\gamma^2(m_e + \gamma\cdot p_\parallel)}{(p^2 - m_e^2 + i\epsilon)^2}eB + O(e^2B^2), \tag{7}$$

and $\exp(\frac{-ie}{2}V^\lambda F_{\lambda\kappa}W^\kappa) = 1 - \frac{ie}{2}\left(V^\lambda F_{\lambda\kappa}W^\kappa\right) + O(e^2B^2)$. The above expansions can be used to compute the amplitude M in powers of eB. Indeed, by dimensional analysis, any given power of eB in the expansion of M is accompanied by an equal power of $1/m_e^2$(for $m_e > p$) or $1/p^2$(for $p > m_e$) with p the typical energy scale of external particles. Clearly, for $B \ll B_c \equiv m_e^2/e$, both $(eB/m_e^2)^n$ and $(eB/p^2)^n$(applicable when $p > m_e$) are much smaller than unity.

From Eqs. (2), (7) and the expansion of the phase factor, the amplitude M to the linear order in eB is

$$M = \frac{G_F g_V}{\sqrt{2}}\frac{e\alpha}{4\pi}\bar{u}(p_2)\gamma_\rho(1-\gamma_5)v(p_1)J^\rho, \tag{8}$$

with

$$\begin{aligned}
J^\rho = {} & C_1\left[(\epsilon_1 F\epsilon_2)(k_1^\rho - k_2^\rho)\right] + C_2\left[(\epsilon_1 Fk_1)(k_1\cdot\epsilon_2)k_2^\rho + (\epsilon_1 Fk_1)(k_1\cdot\epsilon_2)k_2^\rho\right] \\
& + C_3\left[(\epsilon_1 Fk_1)\epsilon_2^\rho + (\epsilon_2 Fk_2)\epsilon_1^\rho\right] + C_4\left[(\epsilon_1 Fk_2)(k_1\cdot\epsilon_2)k_1^\rho + (\epsilon_2 Fk_1)(k_2\cdot\epsilon_1)k_2^\rho\right] \\
& + C_5\left[(\epsilon_1 Fk_2)(k_1\cdot\epsilon_2)k_2^\rho + (\epsilon_2 Fk_1)(k_2\cdot\epsilon_1)k_1^\rho\right] + C_6\left[(\epsilon_1 Fk_2)\epsilon_2^\rho + (\epsilon_2 Fk_1)\epsilon_1^\rho\right] \\
& + C_7(k_2\cdot\epsilon_1)(k_1\cdot\epsilon_2)\left[(Fk_1)^\rho + (Fk_2)^\rho\right] + C_8(\epsilon_1\cdot\epsilon_2)\left[(Fk_1)^\rho + (Fk_2)^\rho\right] \\
& + C_9\left[(k_1 Fk_2)(\epsilon_1\cdot\epsilon_2)(k_1^\rho - k_2^\rho)\right] + C_{10}\left[(k_1 Fk_2)(k_2\epsilon_1)(k_1\epsilon_2)(k_1^\rho - k_2^\rho)\right] \\
& + C_{11}\left[(k_1 Fk_2)(k_2\cdot\epsilon_1\epsilon_2^\rho + k_1\cdot\epsilon_2\epsilon_1^\rho)\right],
\end{aligned} \tag{9}$$

where $C_1, C_2\cdots, C_{11}$ are linear combinations of the integrals $I[a,b,c] = \int_0^1 dx\int_0^x dy\frac{x^b y^{a-b}}{(1-txy-i\varepsilon)^c}$ with $t = 2k_1\cdot k_2/m_e^2$. The detailed structures of these coefficients will be presented elsewhere [9]. We have checked our result by taking the limit $2k_1\cdot k_2/m_e^2 \ll 1$. It agrees with the result of Ref. [6], which is obtained via the effective-Lagrangian approach.

From Eqs. (8) and (9), we can calculate the cross section for $\gamma\gamma \to \nu\bar{\nu}$ in a background magnetic field. For simplicity, let us take the momenta of incoming photons to be along $+z$ and $-z$ directions respectively, with equal magnitudes. The result for $\sigma_B(\gamma\gamma \to \nu\bar{\nu})$ with $B = 0.1\ B_c$ and $\vec{B}$ perpendicular to the collision axis is plotted in Fig. 2. For other relative alignments between $\vec{B}$ and the collision axis, the cross section σ_B varies by no more than an order of magnitude. To explore the validity of the effective-Lagrangian approach, we also plot the cross section $\sigma_B^*(\gamma\gamma \to \nu\bar{\nu})$ obtained in this method [6]. It is found that σ_B and σ_B^* agree reasonably well at a small incoming photon energy (ω), i.e., $\omega/m_e < 0.5$. For ω slightly greater than m_e, the internal electron could become on shell, and σ_B would dominate over σ_B^* due to the rescattering effect by $e^+e^- \to \nu\bar{\nu}$. Such a dominance lasts till $\omega/m_e = 2.2$ where σ_B^* begins to overtake σ_B. Finally, for comparisons, we also display the $2 \to 3$ scattering cross section $\sigma(\gamma\gamma \to \nu\bar{\nu}\gamma)$ obtained in Refs. [10,11]. For $\omega/m_e < 5$, this cross section is seen to be suppressed compared to $\sigma_B(\gamma\gamma \to \nu\bar{\nu})$. At higher energies, it becomes equally important as the latter.

The stellar energy-loss rate Q due to $\gamma\gamma \to \nu\bar{\nu}$ in a background magnetic field has been calculated [6]. We repeat the calculation using our updated result of $\sigma_B(\gamma\gamma \to \nu\bar{\nu})$. The temperature dependencies of Q are listed in Table I. For comparisons, we also list corresponding results obtained from the effective-Lagrangian approach [12]. For temperatures below 0.01 MeV, the effective-Lagrangian approach works very well. On the other hand, this approach becomes rather inaccurate for temperatures greater than 1 MeV. At $T = 0.1$

MeV, our exact calculation gives an energy-loss rate almost two orders of magnitude greater than the result from the effective Lagrangian. Such a behavior can be understood from the energy dependence of the scattering cross section, as shown in Fig. 2. It is clear that, for $T = 0.1$ MeV, Q must have received significant contributions from scatterings with $\omega \approx m_e$. At this energy, the full calculation gives a much larger scattering cross section than the effective Lagrangian does.

By comparing the predictions of the full calculation and the effective-Lagrangian approach [6], we conclude that the applicability of the latter to the energy-loss rate is quite restricted. While the effective Lagrangian works reasonably well with $\omega < 0.1 m_e$, it would give a poor approximation on Q unless $T < 0.01 m_e$.

Besides $\gamma\gamma \to \nu\bar{\nu}$, the crossed processes $\nu(\bar{\nu})\gamma \to \nu(\bar{\nu})\gamma$ and $\nu\bar{\nu} \to \gamma\gamma$ in a background magnetic field also play some roles in astrophysics. For example, one expects that these two processes might be relevant for the mean free paths of supernova neutrinos. In fact, it was recently suggested that [13], for supernova neutrinos, the $2 \to 3$ scatterings $\nu\gamma \to \nu\gamma\gamma$ and $\nu\bar{\nu} \to \gamma\gamma\gamma$ give neutrino mean free paths less than the supernova core radius. Thus they could affect the supernova dynamics. Now since the magnetic field inside the supernova core is typically around $10^{12} G \approx 0.1 B_c$, the cross sections $\sigma_B(\nu(\bar{\nu})\gamma \to \nu(\bar{\nu})\gamma)$ and $\sigma_B(\nu\bar{\nu} \to \gamma\gamma)$ are expected to be comparable to those of $2 \to 3$ scattering just mentioned. Hence one might conclude that $\nu(\bar{\nu})\gamma \to \nu(\bar{\nu})\gamma$ and $\nu\bar{\nu} \to \gamma\gamma$ are also relevant for the supernova dynamics. To examine this statement, one should note that the result of Ref. [13] is based upon extrapolating the energy dependencies of $\sigma(\nu\gamma \to \nu\gamma\gamma)$ and $\sigma(\nu\bar{\nu} \to \gamma\gamma\gamma)$ obtained in the low energy limit $E_\nu,\ E_\gamma \ll m_e$ [5] to energies greater than few times of m_e. Naturally, such an extrapolation is likely to overestimate the cross sections at higher energies, resulting into an underestimation of the corresponding neutrino mean free paths. With this precaution in mind, we shall first compute $\sigma_B(\nu(\bar{\nu})\gamma \to \nu(\bar{\nu})\gamma)$, $\sigma_B(\nu\bar{\nu} \to \gamma\gamma)$ and their corresponding neutrino mean free paths. The mean free paths due to $2 \to 3$ scatterings can then be easily inferred. Hence the results of Ref. [13] can be checked.

The amplitude for $\gamma\nu \to \gamma\nu$ can be inferred from Eqs. (8) and (9) with $v(p_1) \to u(p_1)$ and $k_1 \to -k_1$. It is worth noting that, unlike $\gamma\gamma \to \nu\bar{\nu}$, this process develops no imaginary part since there are no intermediate states available for the rescattering. In Fig. 3, we show the cross sections of $\gamma\nu \to \gamma\nu$ as a function of the incoming photon energy in the center of momentum frame. We have presented two cross sections with the magnetic field parallel and perpendicular to the collision axis respectively. For most incoming photon energies, these two cross sections, denoted as $\sigma_B(\gamma\nu \to \gamma\nu)_\parallel$ and $\sigma_B(\gamma\nu \to \gamma\nu)_\perp$ respectively, differ by no more than an order of magnitude. For comparisons, we also display the $2 \to 3$ scattering cross section $\sigma(\gamma\nu \to \gamma\gamma\nu)$ [10,11]. It is clear that the $2 \to 2$ cross section with $B = 0.1\, B_c$ is significantly greater than the $2 \to 3$ cross section for $\omega \leq m_e$. These two cross sections become comparable for $\omega > m_e$. At $\omega = m_e$, we have, for example, $\sigma_B(\gamma\nu \to \gamma\nu)_\parallel = 1.6 \times 10^{-53}\,\mathrm{cm}^2$, and $\sigma(\gamma\nu \to \gamma\gamma\nu) = 1 \times 10^{-55}\,\mathrm{cm}^2$. For $\omega = 50\ m_e$, both cross sections reach to roughly $10^{-49}\,\mathrm{cm}^2$. We also note that $\sigma_B(\gamma\nu \to \gamma\nu)_{\parallel(\perp)}$ is a smooth function of ω for the energy range considered here. In fact, the cross section maintains such a smooth behavior until ω approaches to m_W.

The neutrino mean free path implied by the above $\nu\gamma$ scattering, which we denote as λ_1, can be calculated using $\lambda_1 = 1/n_\gamma \sigma_{\nu\gamma}$, where n_γ is the photon number density, and $\sigma_{\nu\gamma}$ is the average neutrino-photon scattering cross section. Since we simply concern the order

of magnitude of λ_1, we shall assume the momenta of the photon and the neutrino to be along $+z$ and $-z$ directions respectively, while $\vec{B}$ is taken to be parallel to the collision axis. The neutrino mean free paths for different neutrino energies are summarized in Table II. For $T = 20$ MeV, $E_\nu = 20$ MeV, $\mu_\nu = 0$(a vanishing neutrino chemical potential) and $B = 0.1\, B_c$, we find $\lambda_1 = 3 \times 10^{14}$ cm, which is much greater than 10^6 cm, the supernova core radius. The neutrino mean free path decreases to 4×10^{13} cm for $E_\nu = 50$ MeV, and increases to 1×10^{17} cm for $E_\nu = 1$ MeV. Clearly the photon medium in the supernova is transparent to the neutrino as far as the scattering $\nu\gamma \to \nu\gamma$ is concerned. Hence this process is not expected to affect the supernova dynamics. Furthermore, since the cross section $\sigma(\nu\gamma \to \nu\gamma\gamma)$ is at most comparable to $\sigma_B(\nu\gamma \to \nu\gamma)_{\parallel(\perp)}$, the neutrino mean free path implied by the former process should also be much greater than the supernova core radius. This is in a sharp contrast to the small neutrino mean free path ($\lambda_{\nu\gamma\to\nu\gamma\gamma} \approx 10^{-3}$ cm for $T = 20$ MeV, $E_\nu = 20$ MeV, and $\mu_\nu = 0$) obtained in Ref. [13]. This discrepancy confirms that the extrapolation performed in Ref. [13] indeed underestimates the mean free paths of high energy neutrinos with $E_\nu > m_e$.

Now let us turn to the last process, $\nu\bar{\nu} \to \gamma\gamma$ in a background magnetic field. This process behaves rather similarly as the reversed process $\gamma\gamma \to \nu\bar{\nu}$ discussed before. The scattering cross section $\sigma_B(\nu\bar{\nu} \to \gamma\gamma)_{\parallel(\perp)}$ is depicted in Fig. 4. For comparisons, the corresponding $2 \to 3$ cross section $\sigma(\nu\bar{\nu} \to \gamma\gamma\gamma)$ [10,11] is also shown. One can see that $\sigma_B(\nu\bar{\nu} \to \gamma\gamma)_{\parallel(\perp)}$ peaks locally in the vicinity of $\omega = m_e$ where the threshold effect of electron pair-production emerges. Furthermore, from $\omega = 0.1\, m_e$ to $\omega = m_e$, the $2 \to 2$ cross section dominates the $2 \to 3$ cross section by a few orders of magnitude. The two curves cross at $\omega \approx 5\ m_e$, at which point the $2 \to 3$ process begins to dominate. At $\omega = m_e$, $B = 0.1\ B_c$, we have, for example, $\sigma_B(\nu\bar{\nu} \to \gamma\gamma)_\parallel = 10^{-49}\mathrm{cm}^2$, and $\sigma(\nu\bar{\nu} \to \gamma\gamma\gamma) = 1.5 \times 10^{-53}\mathrm{cm}^2$ [10,11]. The former cross section becomes $3 \times 10^{-50}\mathrm{cm}^2$ at $\omega = 50\ m_e$ while the latter cross section is roughly an order of magnitude larger. The neutrino mean free path due to $\nu\bar{\nu} \to \gamma\gamma$, which we denote as λ_2, can be calculated using $\lambda_2 = 1/n_{\bar{\nu}}\sigma_{\nu\bar{\nu}}$, where $n_{\bar{\nu}}$ is the number density of the antineutrino, and $\sigma_{\nu\bar{\nu}}$ is the average cross section of $\nu\bar{\nu} \to \gamma\gamma$. The results on λ_2 for different neutrino energies are listed in Table II. For $T = 20$ MeV, $E_\nu = 20$ MeV, $\mu_\nu = 0$ and $B = 0.1\, B_c$, we find $\lambda_2 = 5 \times 10^{16}$ cm. The neutrino mean free path decreases to 3×10^{15} cm for $E_\nu = 50$ MeV, and increases to 3×10^{18} cm for $E_\nu = 1$ MeV. Once again, the above neutrino mean free paths are all much greater than the supernova core radius. Furthermore, by comparing $\sigma(\nu\bar{\nu} \to \gamma\gamma\gamma)$ with $\sigma_B(\nu\bar{\nu} \to \gamma\gamma)_{\parallel(\perp)}$, we conclude that the neutrino mean free path relevant to the former process should also be much greater than the supernova core radius. This is again in a sharp contrast to a small neutrino mean free path ($\lambda_{\nu\bar{\nu}\to\gamma\gamma\gamma} \approx 10^{-3}$ cm for $T = 20$ MeV, $E_\nu = 20$ MeV, and $\mu_\nu = 0$) obtained in Ref. [13]. Once more, this discrepancy is due to the cross section extrapolation performed in Ref. [13].

In conclusion, we have illustrated the weak-field expansion technique for processes occurring in a background magnetic field. Specifically, we apply this technique to calculate the cross sections of $\gamma\gamma \to \nu\bar{\nu}$, $\gamma\nu \to \gamma\nu$, and $\nu\bar{\nu} \to \gamma\gamma$ under a background magnetic field. We found that the effective-Lagrangian approach is inappropriate for computing the stellar energy-loss rate due to $\gamma\gamma \to \nu\bar{\nu}$, unless the star temperature is less than $0.01\, m_e$. We also found that the neutrino mean free paths relevant to $\gamma\nu \to \gamma\nu$ and $\nu\bar{\nu} \to \gamma\gamma$ in a background magnetic field are much greater than the supernova core radius. The same conclusions are reached for the neutrino mean free paths relevant to $\gamma\nu \to \gamma\gamma\nu$ and $\nu\bar{\nu} \to \gamma\gamma\gamma$. Therefore

both neutrino-photon scatterings and neutrino-antineutrino annihilations into photons are not expected to affect the supernova dynamics.

ACKNOWLEDGMENTS

This work was supported in part by the National Science Council of R.O.C. under the Grant Nos. NSC-88-2112-M-009-001, NSC-88-2112-M-009-002, and NSC-88-2112-M001-042.

REFERENCES

[1] For a comprehensive review, see G. G. Raffet, *Stars as Laboratories for Fundamental Physics* (University of Chicago Press, Chicago, 1996).

[2] G. G. Raffet, Astrophys. J., **365**, 559 (1990).

[3] P. B. Pal and L. Wolfenstein, Phys. Rev. D **25**, 766 (1982).

[4] M. Gell-Mann, Phys. Rev. Lett. **6**, 70 (1961).

[5] D. A. Dicus and W. W. Repko, Phys. Rev. Lett. **79**, 569 (1997).

[6] R. Shaisultanov, Phys. Rev. Lett. **80**, 1586 (1998).

[7] J. Schwinger, Phys. Rev. **82**, 664 (1951).

[8] A. Chodos, K. Everding, and D. A. Owen, Phys. Rev. D **42**, 2881 (1990).

[9] T.-K. Chyi, C.-W. Hwang, W. F. Kao, G.-L. Lin, K.-W. Ng, and J.-J. Tseng, in preparation.

[10] D. A. Dicus, C. Kao, and W. W. Repko, Phys. Rev. D **59**, 013005 (1999).

[11] A. Abada, J. Matias, and R. Pittau, Nucl. Phys. B **543**, 255 (1999).

[12] In the low temperature limit, i.e., $T \ll m_e$, our Q differs from that of Ref. [6], but the discrepancy is within one order of magnitude.

[13] M. Harris, J. Wang, and V. Teplitz, Report No. astro-ph/9707113.

TABLES

TABLE I. The temperature dependence of energy-loss rate(erg/s = cm^3) by $\gamma\gamma \to \nu\bar{\nu}$ in a background magnetic field. The results given by the effective Lagrangian and our exact calculations are both listed. We take $B = B_c/10$.

Q/T(MeV)	0.001	0.01	0.1	1	10
Exact	1.2×10^{-18}	1.2×10^{-5}	5.6×10^{9}	1.7×10^{18}	3.1×10^{26}
Effective	1.2×10^{-18}	1.2×10^{-5}	1.2×10^{8}	1.2×10^{21}	1.2×10^{34}

TABLE II. The neutrino mean free paths $\lambda_{1,2}$ relevant to the scatterings $\nu\gamma \to \nu\gamma$ and $\nu\bar{\nu} \to \gamma\gamma$ respectively in a background magnetic field $B = B_c/10$. We fix $T = 20$ MeV, $\mu_\nu = 0$ and vary the neutrino energy E_ν from 0.01 MeV to 50 MeV.

E_ν(MeV)	0.01	0.1	1	5	20	50
λ_1 (cm)	1×10^{22}	2×10^{19}	1×10^{17}	5×10^{15}	3×10^{14}	4×10^{13}
λ_2 (cm)	2×10^{21}	1×10^{17}	3×10^{18}	1×10^{18}	5×10^{16}	3×10^{15}

FIGURES

FIG. 1. Feynman diagrams contributing to $\gamma\gamma \to \nu\bar{\nu}$.

FIG. 2. $\sigma_B(\gamma\gamma \to \nu\bar{\nu})$ is the cross section obtained from the exact calculation, while $\sigma_B^*(\gamma\gamma \to \nu\bar{\nu})$ is obtained from the effective Lagrangian approach. The magnetic field direction is taken to be parallel to the collision axis. For comparison, the $2 \to 3$ cross section $\sigma(\gamma\gamma \to \nu\bar{\nu}\gamma)$ is also displayed.

FIG. 3. The solid line and the dotted line depict cross sections $\sigma_B(\gamma\nu \to \gamma\nu)_\perp$ and $\sigma_B(\gamma\nu \to \gamma\nu)_\parallel$ respectively. The dashed line depicts the cross section $\sigma(\gamma\nu \to \gamma\gamma\nu)$.

FIG. 4. The solid line and the dotted line depict cross sections $\sigma_B(\nu\bar{\nu} \to \gamma\gamma)_\perp$ and $\sigma_B(\nu\bar{\nu} \to \gamma\gamma)_\parallel$ respectively. The dashed line depicts the cross section $\sigma(\nu\bar{\nu} \to \gamma\gamma\gamma)$.

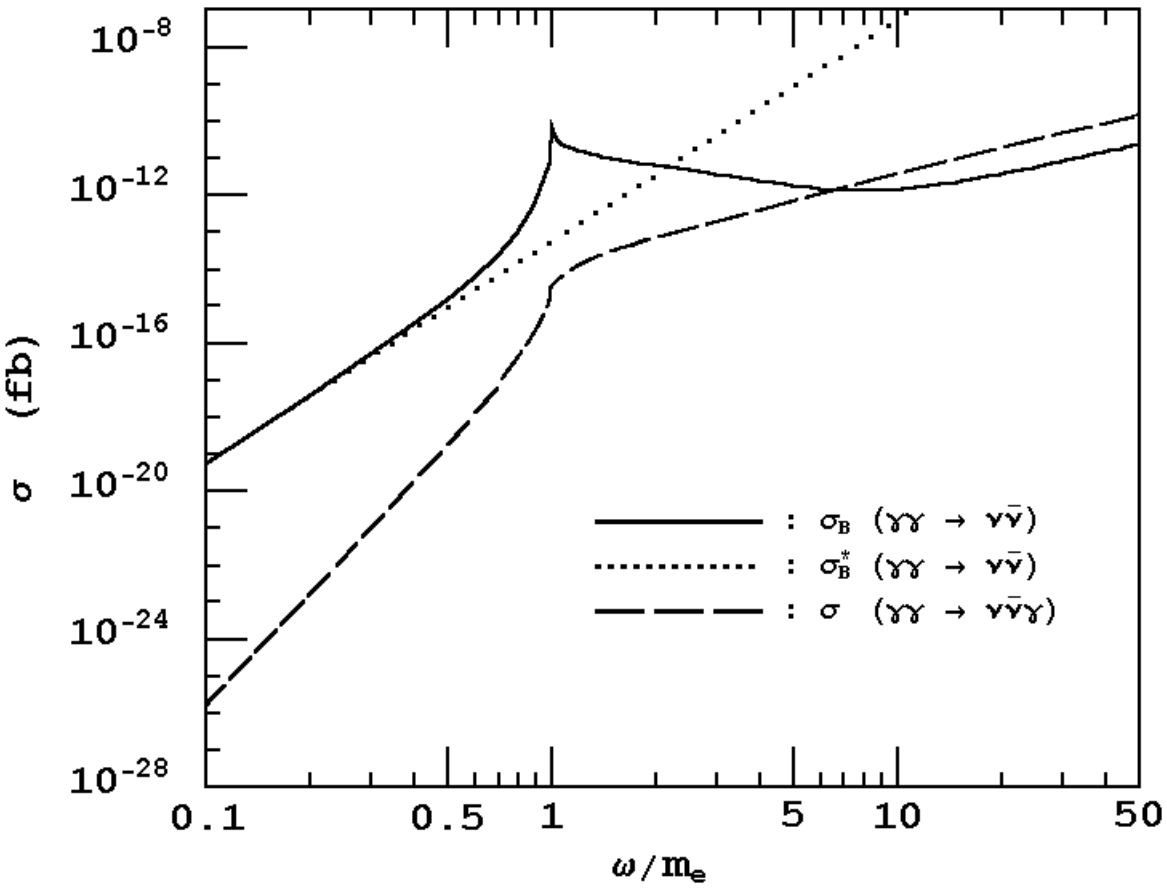
10^{-8}
10^{-12}
10^{-16}
10^{-20}
10^{-24}
10^{-28}
σ (fb)
0.1
0.5
1
5
10
50
ω/m_e
: σ_B (γγ → νν̄)
: σ*_B (γγ → νν̄)
: σ (γγ → νν̄γ)

Fig. 2

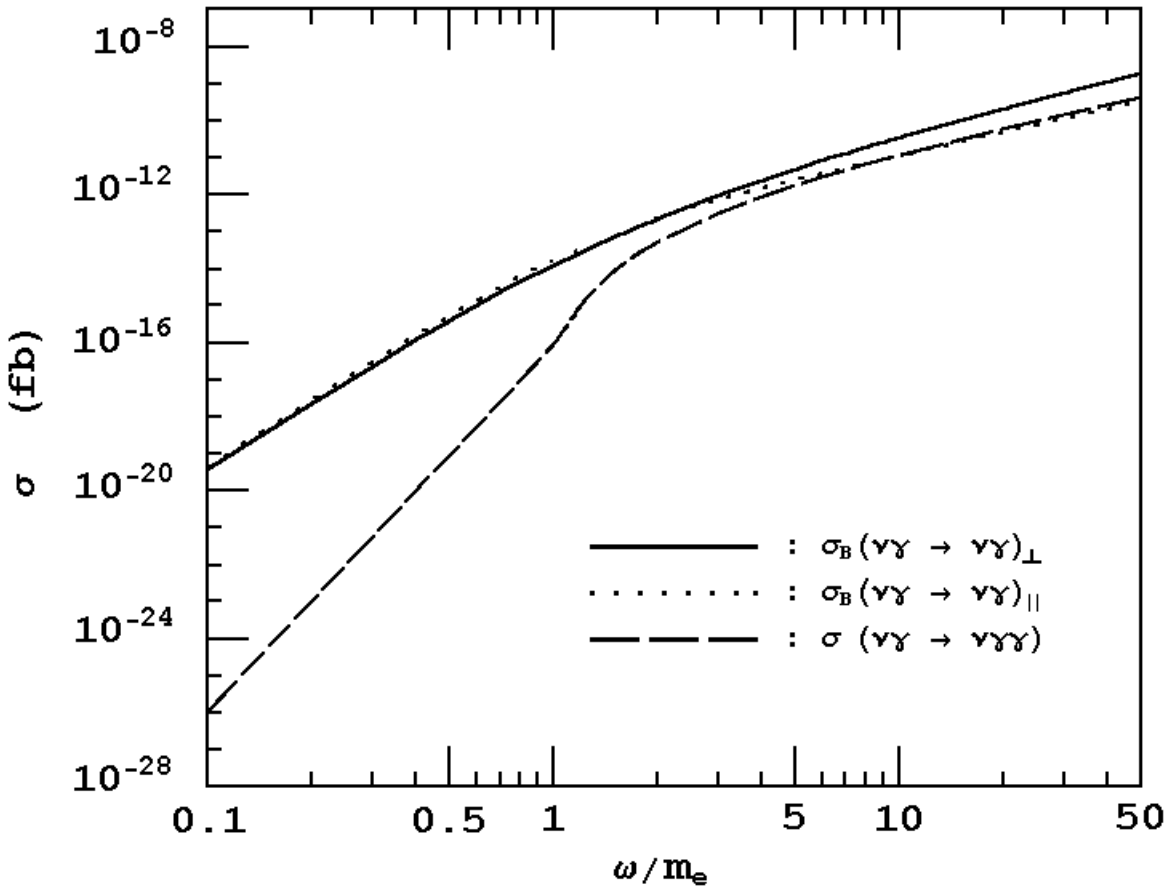
10^{-8}
10^{-12}
10^{-16}
10^{-20}
10^{-24}
10^{-28}
σ (fb)
0.1
0.5
1
5
10
50
ω/m_e
: $\sigma_B(\nu\gamma \to \nu\gamma)_\perp$
: $\sigma_B(\nu\gamma \to \nu\gamma)_{||}$
: $\sigma\ (\nu\gamma \to \nu\gamma\gamma)$

Fig. 3

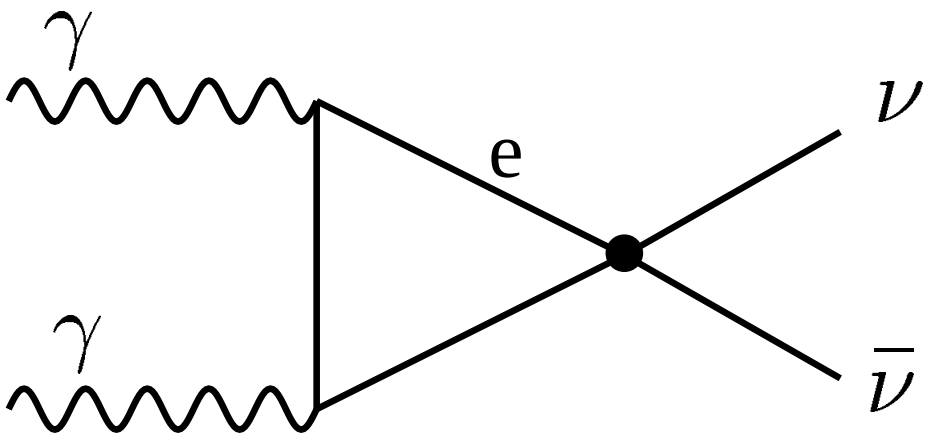

Fig. 1

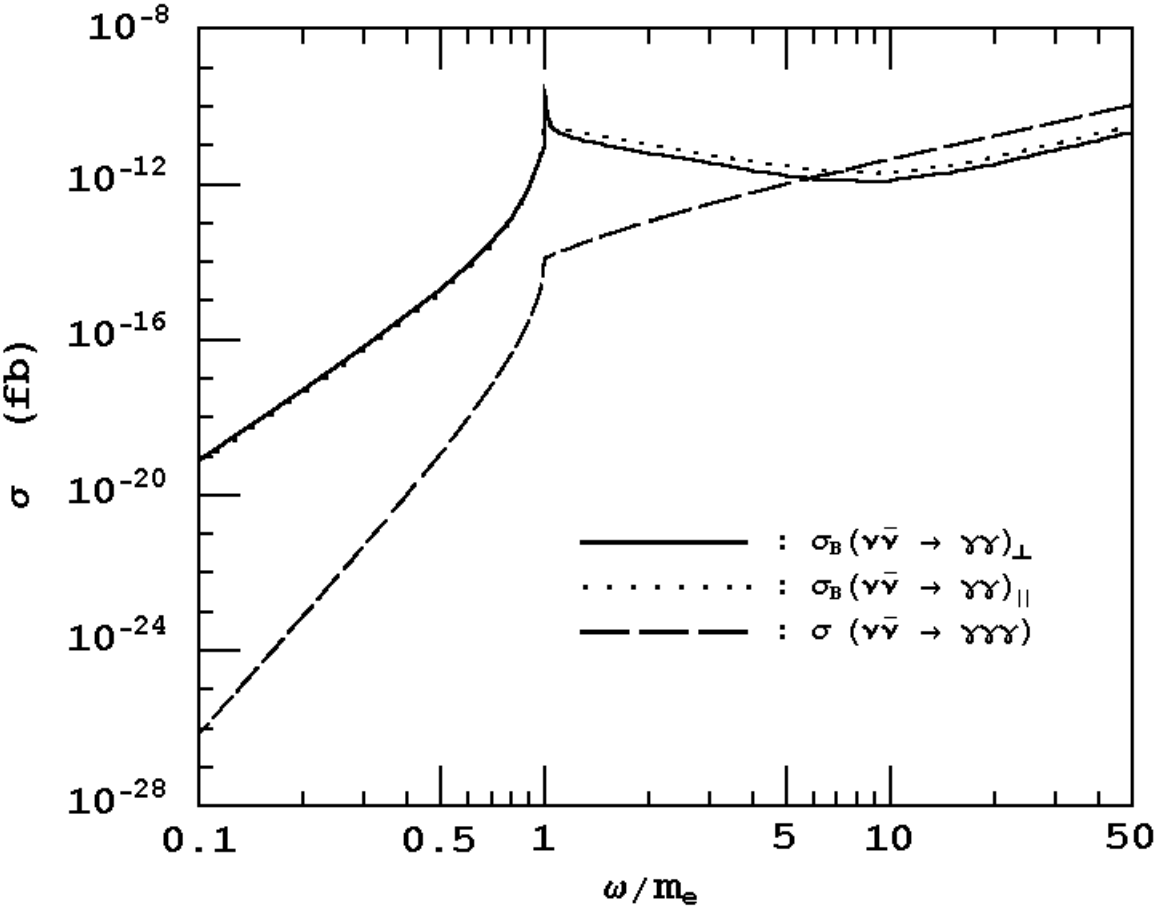
10^{-8}
10^{-12}
10^{-16}
10^{-20}
10^{-24}
10^{-28}
σ (fb)
0.1
0.5
1
5
10
50
ω/m_e
: $\sigma_B(\nu\bar{\nu} \to \gamma\gamma)_\perp$
: $\sigma_B(\nu\bar{\nu} \to \gamma\gamma)_{||}$
: $\sigma\ (\nu\bar{\nu} \to \gamma\gamma\gamma)$

Fig. 4